The Secular Evolution of Disk-Planet and Ring-Satellite Systems

Joseph M. Hahn
Lunar and Planetary Institute

Edoardo Gallo
Harvard University

1 Introduction

The following considers the secular evolution of a handful of perturbers as they interact with a broad disk of particles. This process is modeled by treating the disk as a set of nested gravitating rings whose mutual perturbations cause the rings to flex and tilt over time. The system's secular evolution is then governed by the the classical Laplace–Lagrange secular solution which yields the systems orbit elements $(e, \tilde{\omega}, i, \Omega)$ over time (Murray and Dermott 1999). The main advantage of this approach is that it is fully analytic so it rapidly provides the system's evolution. However there are limitations in our current implementation, namely, that the the e and $\tilde{\omega}$ evolution break down when adjacent rings enter crossing orbits. These limitations are described further in Section 4, as well as forthcoming improvements to the model that will avoid this difficulty.

Two applications of the model are considered here: (*i.*) the primordial Kuiper Belt and (*ii.*) Saturn's rings.

2 The Kuiper Belt

The dots in Fig. 1 indicate the Kuiper Belt Objects (KBOs) eccentricities e and inclinations i plotted versus their semimajor axes a. One plausible explanation for the many Plutinos that inhabit Neptune's 3:2 resonance at $a = 39.5$ AU is that Neptune's early orbit had expanded outwards by $\Delta r \sim 7$ AU as it began to scatter the local planetesimal debris. This outwards expansion would cause Neptune's advancing mean–motion resonances to accumulate numerous KBOs at resonance, which would also pump the trapped KBOs' eccentricities up to the observed values (Malhotra 1995). Although this scenario neatly explains the orbital properties of the KBOs at Neptune's 3:2 resonance, planet migration is rather ineffective at exciting inclinations among the Main Belt KBOs that inhabit the $40 \lesssim a \lesssim 50$ AU zone. These KBO's high inclinations of $i \sim 10^\circ$ (see Fig. 1) thus suggest that another mechanism was also responsible for having stirred up the Kuiper Belt. The following applies the rings model to this environment to see if secular perturbations from the giant planets might also be responsible for disturbing the Kuiper Belt.

2.1 Initial Conditions

Although the current Kuiper Belt has a mass of $M_{\text{KB}} \sim 0.2$ M$_\oplus$ in the $30 < r < 50$ AU interval (Jewitt *et al.* 1998), accretion models tell us that the primordial Kuiper Belt had an initial mass of $M_{\text{KB}} \sim 30$ M$_\oplus$, and that collisions have since depleted the Kuiper Belt mass by a factor of ~ 150 (Kenyon and Luu 1999). In light of this, the following considers the secular evolution of six model Kuiper Belts having masses $M_{\text{KB}} = 0, 0.04, 0.2, 2, 10,$ and 30 M$_\oplus$. All rings are initially in circular orbits coplanar with the invariable plane, and the giant planets have their current masses and orbits.

2.2 Kuiper Belt Results

In our simulations where the Kuiper Belt mass exceeds $M_{\text{KB}} \geq 0.04$ M$_\oplus$, we find that the giant planets launch spiral waves at the inner Kuiper Belt that propagates outwards (see Fig. 2). These waves have the following properties:

- The wavelength is (Ward & Hahn 1998, Tremaine 2001)

$$\lambda \simeq 2\pi \left(\frac{\pi\sigma r^2}{M_\odot}\right)\left|\frac{n}{s}\right| r \sim 8\left(\frac{M_{\text{KB}}}{M_\oplus}\right) \text{ AU} \qquad (1)$$

  where n and s are the disk's mean–motion and precession rates.

- These spiral waves propagate outwards with a velocity (Toomre 1969)

$$c_g = \left(\frac{\pi\sigma r^2}{M_\odot}\right) V_K \sim 4\times 10^{-6}\left(\frac{M_{\text{KB}}}{M_\oplus}\right) \text{ AU/year} \qquad (2)$$

  where V_K is the Kepler velocity. These waves reflect at the disk's outer boundary and return to the inner Kuiper Belt. Eventually a standing wave is established that precesses in concert with Neptune's longitudes, as anticipated by Ward (2002). The time for waves to propagate a distant Δr is

$$t_{\text{prop}} \sim \frac{\Delta r}{c_g} \sim 5\times 10^6 \left(\frac{\Delta r}{20\text{ AU}}\right)\left(\frac{M_{\text{KB}}}{M_\oplus}\right)^{-1} \text{ years.} \qquad (3)$$

- the mean inclination is $\bar{i} \sim 2(M_{\text{KB}}/M_\oplus)^{-2/3}$ degrees while the instantaneous i's range over $0 \lesssim i \lesssim 2\bar{i}$. Thus a lower–mass Kuiper Belt tends to be more strongly disturbed, as is seen in Fig. 1 which shows that these waves could have excited inclinations of $i \sim 10^\circ$ in the current Kuiper Belt which has a mass $M_{\text{KB}} \sim 0.2$ M$_\oplus$.

- The orbits of adjacent rings start to cross when the Kuiper Belt mass is less than $M_{\text{KB}} \lesssim 2$ M$_\oplus$, whereupon the model's e and $\tilde{\omega}$ evolution becomes suspect (see Section 4).

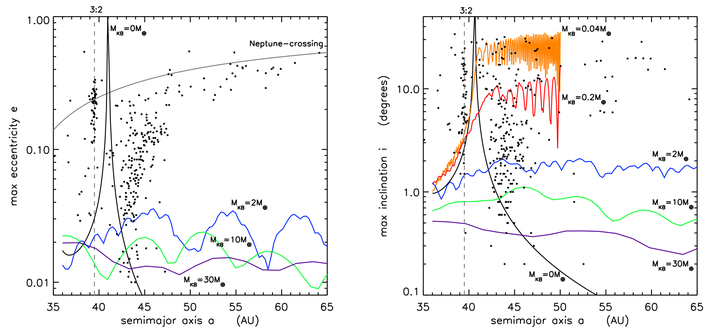

Figure 1: The dots indicate the observed Kuiper Belt eccentricities e and inclinations i while the curves indicate maximum e's and i's obtained by models having a variety of Kuiper Belt masses M_{KB}.

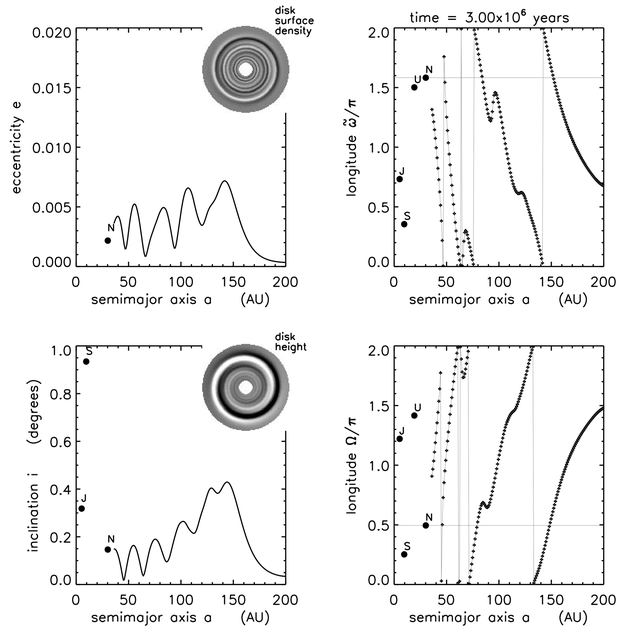

Figure 2: A snapshot of the $M_{\text{KB}} = 10$ M$_\oplus$ system's orbit elements. Greyscales indicate fractional changes of $\pm 20\%$ in the disk surface density and ± 1 AU in the disk's vertical displacement.

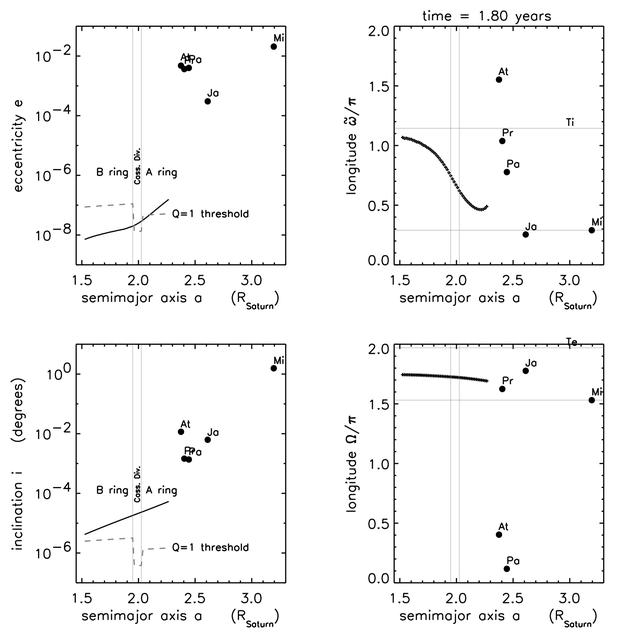

Figure 3: A snapshot of Saturn's rings' orbit elements that are forced by the satellites and the Sun. Dots represent the inner satellites' orbits. The dashed curves indicate the threshold where Toomre's gravitational parameter $Q = cn/\pi G\sigma = 1$. Gravitational stability requires the particles random velocities c to exceed the indicated threshold (Toomre 1964), so the B ring's forced eccentricities will be washed out by the particles' random motions.

3 Saturn's Rings

The rings model is also applied to Saturn's rings to see if these waves might propagate in this system. The model includes the perturbations from the major satellites, the Sun, and Saturn's oblateness. The rings' initial orbit elements are their forced values.

If these waves do indeed propagate in Saturn's rings, we have not yet managed to resolve them. Instead, the rings appear to behave as if they are massless. A snapshot of the system's forced orbits are shown in Fig. 3. Note that the forced eccentricities in the B ring are smaller than the minimum required by gravitational stability (e.g., they are below the $Q = 1$ threshold of Fig. 3), so these motions are washed out by the particles' random motions.

It is interesting to note that the A ring's longitudes $\tilde{\omega}$ precess in concert with Mimas while the B ring precesses at Titan's rate that is about 140 times slower. However the radius where the rings' precession rate $\dot{\tilde{\omega}}$ switches from Titan's to Mimas control, r_c, drifts with time over $1.85 \lesssim r_c \lesssim 2.05$ Saturn radii. This interval also spans the Cassini Division, which is indicated by the shaded region in Fig. 4. Although this might be a mere coincidence of features, we are also exploring whether this break in precession rates near the A/B ring boundary might also promote particle collisions that could sustain the broad gap at the Cassini Division.

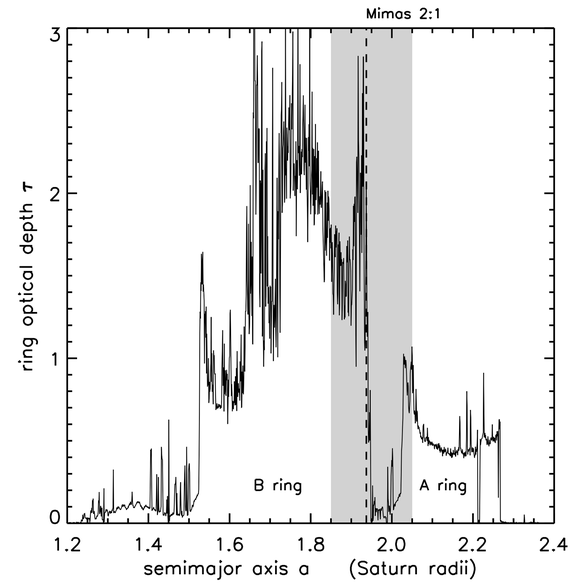

Figure 4: Saturn's rings' normal optical depth τ versus distance a (kindly provided by Mark Showalter/PDS Rings Node). The shaded region indicates the zone swept by the 'control radius' r_c, which is the radius where the rings' periapse precession rates change from the control of Titan to Mimas.

4 Model Limitations and Future Developments

The equations of motion for the system's e and $\tilde{\omega}$ evolution break down when adjacent rings enter crossing orbits; this occurs when the Kuiper Belt mass is $M_{\text{KB}} \lesssim 2$ M$_\oplus$. The problem is that our current implementation does not account for a ring's finite thickness h that results from the particles' dispersion velocities. However this is readily handled by first softening the rings' gravitational potentials over the ring thickness h and then re–deriving the equations of motion (see Tremaine 2001); this will be accounted for in the next generation of the rings model. Note, however, that the i and Ω evolution reported here is still reliable provided the disk scale height h is small compared to the radial wavelength λ.

Note also that the simple model employed here does not account for other "long–period" terms in the equation of motion, as well the effects due to the precession of Saturn's pole, which contribute further to the rings' forced motions at Saturn (c.f., Burns *et al.* 1979).

5 References

Burns, Hamill, Cuzzi, and Durisen, 1979, AJ, 84, 1783
Jewitt, Luu, and Trujillo, 1998, AJ, 115, 2125
Kenyon and Luu, 1999, AJ, 118 1101
Malhotra, 1995, AJ, 110, 420
Murray and Dermott, 1999, Solar System Dynamics
Toomre, 1964, ApJ, 139, 1217
Toomre, 1969, ApJ, 158, 899
Tremaine, 2001, AJ, 121, 1776
Ward, 2002, BAAS, 33, #04.01
Ward and Hahn, 1998, AJ, 116, 489